horticulturae

MDPI

Article

Systematic Characterization of *Brassica napus HIR* Gene Family Reveals a Positive Role of *BnHIR2.7* in *Sclerotinia sclerotiorum* Resistance

Mengqi Li [1,2], Yuqiao Tang [1,2], Mengna Yu [1], Yonghai Fan [1], Shahid Ullah Khan [1,3,*], Wei Chang [1], Xiaodong Li [1], Siyu Wei [1], Lijuan Wei [1,4,5], Cunmin Qu [1,4,5], Jiana Li [1,4,5] and Kun Lu [1,4,5,*]

1 Integrative Science Center of Germplasm Creation in Western China (CHONGQING) Science City and Southwest University, College of Agronomy and Biotechnology, Southwest University, Beibei, Chongqing 400715, China
2 Institute of Innovation and Entrepreneurship, Southwest University, Beibei, Chongqing 400715, China
3 Department of Biochemistry, Women Medical and Dental College, Khyber Medical University, Pesharwar 22080, Pakistan
4 Engineering Research Center of South Upland Agriculture, Ministry of Education, Chongqing 400715, China
5 Academy of Agricultural Sciences, Southwest University, Beibei, Chongqing 400715, China
* Correspondence: shahidbiochem@wmc.edu.pk (S.U.K.); drlukun@swu.edu.cn (K.L.); Tel.: +92-3350955310 (S.U.K.); +86-23-68251264 (K.L.)

Abstract: Hypersensitive-induced response protein (HIR) is a class of plant immune proteins that play pivotal roles in *Sclerotinia sclerotiorum* (Lib.) de Bary resistance. However, there has been no systematic investigation and identification of *HIR* genes in rapeseed (*Brassica napus* L.). Hence, we identified 50 *BnHIR* genes and classified them into four groups. Subcellular localization prediction suggested that HIR proteins are mainly localized in the mitochondria. *Cis*-acting elements involved in light and diverse abiotic stress were found in the promoter regions of *BnHIR*. The majority of *BnHIR* genes in Groups 1/3/4 were expressed in most examined tissues, especially in leaves and siliques pericarp, while the *BnHIR* genes in Group 2 were not or had low expression in all detected tissues. In the case of *S. sclerotiorum* inoculation, *HIR* genes in Groups 1/3/4 were strongly induced, especially homologous genes in Group 1, which exhibited different expression patterns. Moreover, overexpression of *BnHIR2.7* in *Arabidopsis thaliana* illustrated its prominent resistance to *S. sclerotiorum*. Our study provides insight into the evolutionary relationships of the *HIR* family genes in *B. napus* and lays the foundation for their resistance to *S. sclerotiorum* in *B. napus*.

Keywords: hypersensitive-induced response protein; *Brassica napus*; expression patterns; *Sclerotinia sclerotiorum inoculation*

Citation: Li, M.; Tang, Y.; Yu, M.; Fan, Y.; Khan, S.U.; Chang, W.; Li, X.; Wei, S.; Wei, L.; Qu, C.; et al. Systematic Characterization of *Brassica napus HIR* Gene Family Reveals a Positive Role of *BnHIR2.7* in *Sclerotinia sclerotiorum* Resistance. *Horticulturae* **2022**, *8*, 874. https://doi.org/10.3390/horticulturae8100874

Academic Editor: Francesco Faretra

Received: 14 August 2022
Accepted: 19 September 2022
Published: 23 September 2022

1. Introduction

Sclerotinia Disease (SD) is a host non-specific soil-borne fungal disease mainly caused by *Sclerotinia sclerotiorum* (Lib.) de Bary. After completing one life cycle, the fungus can remain active for decades by producing long-lived dormant bodies or sclerotia to exacerbate the potential SD inoculum [1]. SD is a potential problem that threatens multiple traits in *Brassica napus* L., such as reducing oil content, changing fatty acid composition, and fungal toxicity, which seriously affects the quality of rapeseed oil and causes substantial economic losses. Although traditional fungicides have a certain positive effect on SD control, the host range of *S. sclerotiorum* still exists widely due to its long-lived capacity in soil. Therefore, breeding new varieties is highly urgent to resist *S. sclerotiorum* in rapeseed [2].

The influence of pathogenic bacteria or the stress of unfavorable environmental conditions can stimulate plant hypersensitive reactions (HR). Hypersensitive-induced reaction (HIR) is involved in plant HR as a hypersensitivity protein [3]. HIR proteins are a class of hypersensitive reactions (HR). These proteins are part of the PID (proliferation, ion, and

death) superfamily, and contain the stomatin/prohibitin/flotillin/HflK (SPFH) domain, which may play an important part in cell proliferation, ion channel regulation, and cell death [4–6]. The HIR protein induces programmed cell death in the lesions by mediating the HR response, thereby inhibiting the further spread of *S. sclerotiorum* hyphae. In plants, HIR genes are divided into four groups [7]. All four groups of *HIR* genes in *A. thaliana* are expressed in leaves, but their abundance varies. Moreover, all AtHIR proteins are enriched in the membrane microdomain of the plasma membrane and form both homo- and hetero-oligomers in vivo [8]. It was found that in rice, *OsHIR1* binds to the plasma membrane and triggers hypersensitive cell death. Pathogen inoculation studies of transgenic *A. thaliana* heterologously expressing *OsHIR1* showed that all transgenic lines exhibited enhanced resistance to *Pseudomonas syringae* pv *tomato* DC3000 (*Pst* DC3000) [9]. In wheat (*Triticum aestivum* L.), expression of *TaHIR1* and *TaHIR3* decreased under environmental stimuli such as low temperature, drought, and high salt stress [10].

In addition, *HIR* genes have been identified and studied in many species, including tobacco (*Nicotiana tabacum* L.) [11], maize (*Zea mays* L.) [12], barley (*Hordeum vulgare* L.) [13], pepper (*Piper nigrum* L.) [14], and wheat [10]. *B. napus* is one of the most important allopolyploid crops around the world, originating from *Brassica rapa* L. and *Brassica oleracea* L. [15]. Despite the importance of *Brassica* plants, the identity and function of *BnHIR* genes have not been studied in depth. In this study, we identified *HIR* family genes in *B. napus* using *AtHIR* genes as queries and studied their phylogenetic relationships, gene structures, and *cis*-acting elements. We also analyzed the spatio-temporal expression patterns of the *BnHIR* genes in various tissues during different stages, as well as the expression patterns induced by *S. sclerotiorum*. Moreover, overexpressed *BnHIR2.7* in *Arabidopsis thaliana* (L.) Heynh. showed resistance to *S. sclerotiorum*, which could effectively inhibit the growth of *S. sclerotiorum* in leaves compared with the wild type. These results lay the base for understanding the function of *HIR* genes and the cultivation of Sclerotinia-resistant materials in *B. napus*.

2. Materials and Methods

2.1. Plants, Strain Materials, and Growth Conditions

The *A. thaliana* wild-type Col-0 and *B. napus* variety ZS11 were supplied by Southwest University, China. *A. thaliana* seeds were sterilized and sown on 1/2 Murashige and Skoog (MS) medium for two weeks and then transplanted into nutrient soil to continue culturing in the growth chamber (16 h photoperiod, 25/18 °C when the fourth leaf appeared, day/night, 60% humidity, 250 $\mu mol \cdot m^{-2} \cdot s^{-1}$). The rapeseed was sterilized and sown on MS medium, transplanted into nutrient soil for cultivation after two leaves, and then *S. sclerotiorum* strain 1980 was grown. The sclerotia of *S. sclerotiorum* were sterilized and placed on Potato Dextrose Agar (PDA) medium and cultured in a 23 °C incubator to the third generation.

2.2. Identification of BnHIR Gene Family in B. napus

The genome, coding, and protein sequences of *A. thaliana* and *B. napus* were downloaded from the *Arabidopsis* Information Resource (http://www.arabidopsis.org, accessed on 13 December 2021) and EnsemblPlants (http://plants.ensembl.org, accessed on 13 December 2021), respectively. To identify *HIR* genes in *B. napus*, 18 HIR protein sequences from *A. thaliana* were used as queries in a reciprocal BLASTP [16,17], with a threshold e-value of less than 1×10^{-5}, minimal alignment coverage was 50% [18]. Then, the conserved SPFH domain in HIR candidate proteins was confirmed using the website Pfamscan (https://www.ebi.ac.uk/Tools/pfa/pfamscan/, accessed on 5 February 2022). Protein molecular weight (MW) and theoretical isoelectric point (pI) were predicted by the Prosite ExPASy server (http://web.expasy.org/protp aram/, accessed on 5 February 2022). Transmembrane transit peptides were predicted using the TMpred tool (http://www.ch.embnet.org/software/TMPRED_form.html/, accessed on 7 February 2022), and SignalP5.0 (https://services.healthtech.dtu.dk/service.php?SignalP-5.0, accessed on 5 February 2022) was used to identify signal peptides. The subcellular locations of HIR pro-

teins were predicted by plant mPLoc (http://www.csbio.sjtu.edu.cn/bioinf/plant-multi/, accessed on 20 March 2022) [19].

2.3. Phylogenetic Analysis, Gene Structure, and Protein Motif Analysis

The HIR proteins of *A. thaliana* and *B. napus* were aligned by MUSCLE (multiple sequence comparison of logarithmic expectation, http://www.ebi.ac.uk/Tools/msa/MUSCLE/, accessed on 8 February 2022) [20]. The maximum likelihood (ML) tree was constructed to demonstrate their phylogenetic relationship using the online PhyML server (PhyML3.0, http://www.atgc-montpellier.fr/phyml, accessed on 10 February 2022) [21,22] with the JTT + G+F substitution model. Model of rate heterogeneity: discrete gamma; the number of substitution rate categories, 4; bootstrap replicates, 100. The phylogenetic trees were modified and visualized in Evolview V3 [23]. The intron structure of *BnHIRs* was displayed by the Gene Structure Display Server (GSDS 2.0, http://gsds.gao-lab.org/, accessed on 12 February 2022). The conserved motifs of BnHIR proteins were predicted using MEME (Multiple EM for Motif Elicitation) V5.0.4 (http://alternate.MEME suite.org, accessed on 13 February 2022) [24], with the following parameter settings: the optimal motif width between 6 and 200; the number of motifs 15.; only motifs with E-value lower than 1×10^{-10} were kept for further study.

2.4. Analysis of Cis-Acting Elements and Expression Patterns of BnHIR Genes

The 2000-bp genomic DNA sequence upstream of *BnHIR* genes was extracted using TBtools [25]. Then sequences were submitted to PlantCARE (http://bioinformatics.psb.ugent.be/webtools/PlantCARE/html/, accessed on 17 March 2022) [26] to identify potential *cis*-acting elements and plotted using R package tidyverse. To analyze the expression patterns of *BnHIR* genes at different tissues during different stages, we retrieved their expressions from the BrassicaEDB database (https://biodb.swu.edu.cn/brassica/, accessed on 13 February 2022) [27], including roots (Ro-f), stems (St-f), leaves (LeY-f), buds (Bu-b), petals (Pe-f), seeds (Se), and silique pericarp (SP) collected at 7, 13, 21, 27, 35, 43, and 49 days after pollination (DAP); and seeds coat (SC) and embryo (Em) at 21, 27, 35, and 43 DAP. Moreover, we analyzed *BnHIR* gene expressions after *S. sclerotiorum* infection, and the RNA-seq expression data of *S. sclerotiorum* infection were downloaded from the NCBI SRA database (PRJNA274853) [28]. All expression levels were normalized by $\log_2$ (FPKM + 1) and visualized by TBtools [25].

2.5. Overexpression Vector Construction and Plant Transformation

Total RNA was extracted from the leaves of *B. napus* and *A. thaliana* using an RNA extraction kit (Tiangen, Beijing, China). First-strand cDNA was synthesized using PrimeScript RT Master Mix Kit (TaKaRa, Dalian, China). Total DNA was extracted from *B. napus* and *A. thaliana* leaves using the CTAB method [29].

The coding sequence (CDS) of *BnHIR2.7* was firstly amplified using the primer pair OV-HIR2.7-F/OV-HIR2.7-R and recombined into vector pEarlyGate101 for constructing the overexpression vector, resulting in p35S::BnHIR2.7-YFP (named OV-BnHIR2.7). Then, the transgenic Arabidopsis lines of OV-BnHIR2.7 were acquired through *Agrobacterium tumefaciens*-mediated transformation of strain GV3101 [30]. Primer Premier 5 (https://premierbiosoft.com/index.html) was used to design primers for this experimental step, and the primer sequences are listed in Table S1.

2.6. Phenotypic Observation of A. thaliana Transgenic and Mutant Plants

The *AtHIR* T-DNA insertion mutant (SALK_037519C, named Athir2.7-Mu) was obtained from AraShare (http://www.AraShare.cn, accessed on 20 May 2021). The homozygous Athir2.7-Mu mutants were identified and were screened using primers Athir2.7-LP/Athir2.7-RP and LBb1.3/Athir2.7-RP (Table S1). Total RNA was extracted from leaves of seedlings of Col-0, OV-BnHIR2.7, and Athir2.7-Mu, and first-strand cDNA was synthesized as previously described. qRT-PCR primers were obtained from the qPrimerDB database

(http://biodb.swu.edu.cn/qPrimerDB, accessed on 25 April 2022) for OV-BnHIR2.7 and Athir2.7-Mu [31] (Table S1), and the qRT-PCR reactions were performed according to the MIQE guidelines [32] with three technical replicates per sample. Using the $2^{-\Delta\Delta Ct}$ method, *BnACT7* was used as control for normalization [33].

After qRT-PCR analysis, the OV-BnHIR2.7 line with the highest expression of *BnHIR2.7* and the Athir2.7-Mu line with the lowest expression was selected for phenotype observation. Plant height was measured from the cotyledon nodes to the top of the main inflorescence at maturity. At 50 days of the seedling stage, five siliques from the bottom to the top of the main stem were selected to measure and count the length of the siliques.

2.7. Expression Analysis of BnHIR2.7 under the Infection of S. sclerotiorum

To confirm the function of *BnHIR2.7* to *S. sclerotiorum* resistance, leaves of *A. thaliana* Col-0, OV-BnHIR2.7, and AtHIR2.7-Mu were selected for *S. sclerotiorum* inoculation experiments. Edge hyphae were excised using a 1 mm punch and carefully turned over to the front of normal leaves. The lesion area was measured and photographed every 12 h, with three replicates of each experiment. Each *A. thaliana* plant was inoculated on three leaves, and samples were collected every 12 h and immediately stored in liquid nitrogen. The Col-0, OV-BnHIR2.7, and Athir2.7-Mu leaves that had grown normally for 40 days were selected, and the three inoculated leaves of each treatment were stained with trypan blue to observe the leaf cells. Briefly, a 0.4% trypan blue staining solution was used to immerse leaves in trypan blue dye solution for 36 h and then leaves were decolorized using glacial acetic acid and methanol (3:1, v:v). Moreover, the gene expression levels of some marker genes in the SA and MeJA pathways were identified after inoculation with *S. sclerotiorum*.

2.8. Statistical Analysis

Statistical analysis was performed using SPSS v22.0 and one-way analysis of variance (ANOVA), and results are expressed as mean ± standard error and significant t-test, *, $p < 0.05$; **, $p < 0.01$; ***, $p < 0.001$. Results were visualized using GraphPad Prism 10 software [34].

3. Results

3.1. Identification and Characterization of the B. napus HIR Family

We identified 50 *HIR* genes with the conserved SPFH domain in *B. napus*. The putative HIR genes in *B. napus* were named according to their orthologs in *A. thaliana* (Table 1). Most *AtHIR* genes in *B. napus* have multiple homologous genes, and most *AtHIR* genes in *B. napus* have multiple homologs. However, in the subfamilies *PHB5*, *PHB7*, and *HIR4*, no homologues of *A. thaliana* genes were found in *B. napus*, indicating that the subfamily may have been lost. Among the 50 BnHIR proteins, the lengths ranged from 227 (BnHIR1) to 535aa (BnHIR1.3), and the MW ranged from 25.97 (BnHIR1) to 58.02 kDa (BnHIR1.3). Interestingly, the isoelectric point distribution of BnHIR proteins is wide, ranging from 4.99 (BnHIR1) to 9.55 (BnPHB2.5). Some proteins have transmembrane structures, such as BnPHB1.3, BnPHB1.5, and BnPHB1.7. Subcellular localization indicated that the majority of BnHIR proteins were localized in mitochondria and a few in the nucleus (Table 1).

Table 1. Physical and chemical properties of HIR proteins in *B. napus*.

Gene Name	Gene ID	Homologs in *A. thaliana*	Amino Acids	MW (kDa) [a]	pI [b]	Subcellular Localization
BnHIR5.1	*BnaA02g32070D*	*AT5G25260*	469	51,982.35	5.57	Nucleus
BnHIR5.2	*BnaA02g32090D*	*AT5G25260*	468	51,756.07	5.42	Nucleus
BnHIR5.3	*BnaC02g40750D*	*AT5G25260*	467	51,708.93	5.40	Nucleus
BnHIR6.1	*BnaA02g34440D*	*AT5G64870*	469	51,663.18	6.12	Nucleus
BnHIR6.2	*BnaA06g23810D*	*AT5G64870*	470	51,848.36	5.95	Nucleus
BnHIR6.3	*BnaA07g33580D*	*AT5G64870*	467	51,499.11	6.60	Nucleus

Table 1. *Cont.*

Gene Name	Gene ID	Homologs in *A. thaliana*	Amino Acids	MW (kDa) [a]	pI [b]	Subcellular Localization
BnHIR6.4	*BnaC03g49410D*	*AT5G64870*	470	51,853.33	5.88	Nucleus
BnHIR6.5	*BnaC06g38190D*	*AT5G64870*	469	51,551.08	6.39	Nucleus
BnHIR6.6	*BnaCnng58920D*	*AT5G64870*	345	37,805.16	6.13	Nucleus
BnHIR1	*BnaC09g53100D*	*AT5G62740*	227	25,972.59	4.99	Chloroplast, Nucleus
BnHIR2.1	*BnaA02g35710D*	*AT1G69840*	285	31,218.54	5.49	Mitochondrion
BnHIR2.2	*BnaA03g27520D*	*AT3G01290*	286	31,610.32	5.89	Mitochondrion
BnHIR2.3	*BnaA05g34000D*	*AT3G01290*	286	31,529.24	6.01	Mitochondrion
BnHIR2.4	*BnaA07g28360D*	*AT1G69840*	286	31,316.54	5.27	Mitochondrion
BnHIR2.5	*BnaC03g32530D*	*AT3G01290*	286	31,610.32	5.89	Mitochondrion
BnHIR2.6	*BnaC05g48690D*	*AT3G01290*	286	31,529.24	6.01	Mitochondrion
BnHIR2.7	*BnaC06g30890D*	*AT1G69840*	286	31,316.54	5.27	Mitochondrion
BnHIR2.8	*BnaCnng44030D*	*AT1G69840*	285	31,087.34	5.35	Mitochondrion
BnHIR3.1	*BnaA03g13070D*	*AT5G51570*	292	32,465.11	5.28	Mitochondrion
BnHIR3.2	*BnaC03g15940D*	*AT5G51570*	292	32,366.02	5.38	Mitochondrion
BnPHB1.1	*BnaA01g08360D*	*AT4G28510*	290	32,048.98	9.45	Mitochondrion
BnPHB1.2	*BnaA08g13690D*	*AT4G28510*	242	27,374.50	8.69	Mitochondrion
BnPHB1.3	*BnaA09g19330D*	*AT2G03510*	361	41,160.82	5.44	Mitochondrion
BnPHB1.4	*BnaC01g09910D*	*AT4G28510*	290	32,048.98	9.45	Mitochondrion
BnPHB1.5	*BnaC02g47990D*	*AT2G03510*	347	39,719.46	6.10	Mitochondrion
BnPHB1.6	*BnaC08g13090D*	*AT4G28510*	260	28,591.94	9.06	Mitochondrion
BnPHB1.7	*BnaC09g21530D*	*AT2G03510*	358	40,821.52	5.56	Mitochondrion
BnPHB2.1	*BnaA08g27620D*	*AT1G03860*	288	31,909.77	9.37	Mitochondrion
BnPHB2.2	*BnaA09g50790D*	*AT1G03860*	288	32,033.87	9.39	Mitochondrion
BnPHB2.3	*BnaA10g02220D*	*AT1G03860*	288	31,923.74	9.35	Mitochondrion
BnPHB2.4	*BnaC05g02140D*	*AT1G03860*	288	31,908.68	9.37	Mitochondrion
BnPHB2.5	*BnaC08g00370D*	*AT1G03860*	306	34,181.58	9.55	Mitochondrion
BnPHB2.6	*BnaC08g43560D*	*AT1G03860*	288	31,991.83	9.37	Mitochondrion
BnPHB3.1	*BnaA04g10580D*	*AT5G40770*	277	30,481.01	7.94	Mitochondrion
BnPHB3.2	*BnaA07g15170D*	*AT5G40770*	277	30,446.99	7.94	Mitochondrion
BnPHB3.3	*BnaC04g32860D*	*AT5G40770*	277	30,481.01	7.94	Mitochondrion
BnPHB3.4	*BnaC06g13200D*	*AT5G40770*	277	30,481.01	7.94	Mitochondrion
BnPHB4.1	*BnaA06g32230D*	*AT3G27280*	278	30,372.77	6.94	Mitochondrion
BnPHB4.2	*BnaA09g01960D*	*AT3G27280*	278	30,330.69	6.94	Mitochondrion
BnPHB4.3	*BnaC07g24140D*	*AT3G27280*	278	30,367.75	6.99	Mitochondrion
BnPHB4.4	*BnaC09g01400D*	*AT3G27280*	278	30,330.69	6.94	Mitochondrion
BnHIR7.1	*BnaA01g16560D*	*AT4G27585*	395	43,279.16	6.30	Mitochondrion
BnHIR7.2	*BnaA02g09860D*	*AT4G27585*	404	43,570.06	9.05	Mitochondrion
BnHIR7.3	*BnaA02g09870D*	*AT4G27585*	535	58,018.04	5.71	Nucleus
BnHIR7.4	*BnaA03g12010D*	*AT4G27585*	420	45,807.70	8.50	Mitochondrion
BnHIR7.5	*BnaA10g07200D*	*AT4G27585*	364	39,713.44	8.89	Mitochondrion
BnHIR7.6	*BnaC01g20150D*	*AT4G27585*	398	43,625.71	6.74	Mitochondrion
BnHIR7.7	*BnaC02g13810D*	*AT4G27585*	378	40,677.62	9.13	Nucleus
BnHIR7.8	*BnaC03g14740D*	*AT4G27585*	359	39,006.84	9.02	Mitochondrion
BnHIR7.9	*BnaC02g13820D*	*AT4G27585*	528	57,171.01	5.67	Mitochondrion

[a] MW, molecular weight; [b] pI, isoelectric point.

3.2. Phylogenetic Analysis of HIR Proteins in B. napus

The maximal likelihood (ML) phylogenetic tree containing 68 HIR proteins from *B. napus* (50) and *A. thaliana* (18) was constructed to explore the phylogenetic relationships. The bootstrap value showed that *B. napus* HIR proteins can be divided into four groups: Group 1 (HIR1/2/3/4/7 clade), Group 2 (HIR5/6 clade), Group 3 (PHB1 clade), and Group 4 (PHB2/3/4 clades). Group 1 and Group 4 are the largest clades containing 26 members, and Group 3 is the smallest clade containing 4 members. In particular, HIR5/6 formed an independent clade during evolution, while HIR1/2/3/4/7 became a clade. In addition, some genes in the HIR2 subfamily correspond to *Arabidopsis* AtHIR1, which

then combine to form a larger clade (Figure 1). The evolutionary relationships among the rapeseed HIR genes are consistent with those of *A. thaliana*, except for the BnHIR1 clade.

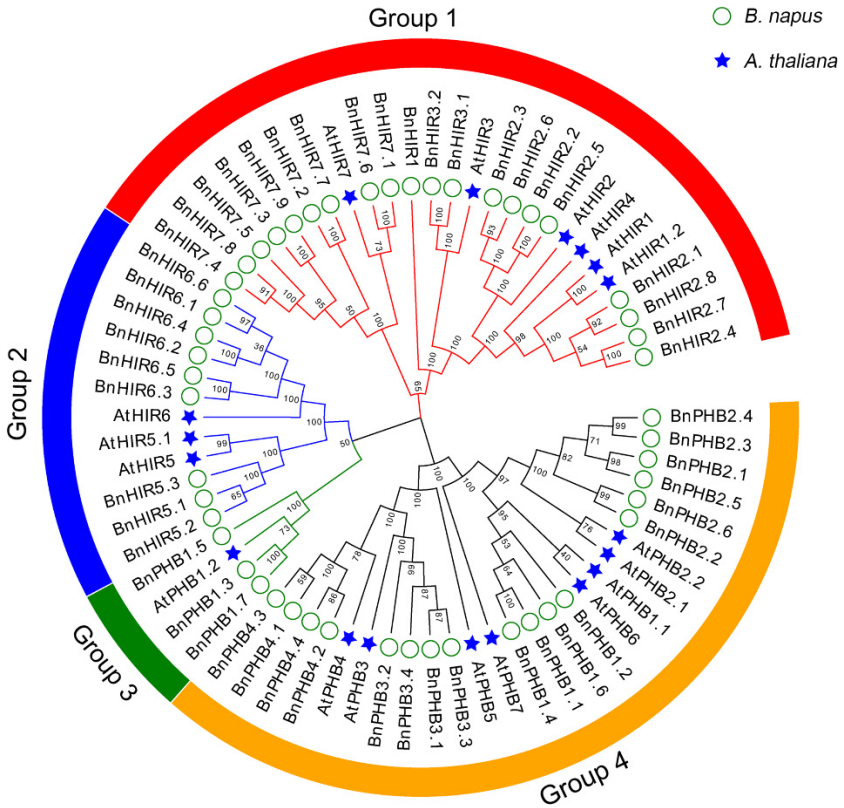

Figure 1. Phylogenetic relationship of HIR proteins between *A. thaliana* and *B. napus*. The ML tree was generated with bootstrap analysis (100 replicates) using the online PhyML server. The tree was visualized by Evolview V3. HIR proteins in the phylogenetic tree clustered into four groups (Groups 1–4). At: *A. thaliana*; Bn: *B. napus*.

3.3. Gene Structure and Conserved Motif Analysis

To analyze the exon/intron structure of the *BnHIR* and *AtHIR* genes, we compared the CDS with their corresponding genomic sequences. The results showed that most *BnHIR* genes contained 3–6 exons, and some genes contained more than 8 exons, such as *BnHIR7* subfamily genes (Figure 2a). Genes from the same subfamily presented similar gene structures. Most *BnHIR* genes have a long exon at the 3′ ends of their genomic sequence. Furthermore, the gene structure of *BnHIR* is highly similar to their corresponding *AtHIR*.

To better investigate structural diversity among BnHIR proteins, MEME was used to analyze 15 conserved motifs identified in the full-length BnHIR protein (Figure 2b). Motif 2 or motif 3 was observed in all 50 BnHIR proteins. Multiple motifs were observed in almost all BnHIR proteins, with some motifs only found in a few HIR proteins, except for BnHIR1 proteins that contain only motif 9. For example, motif 10 was only detected in Group 3, while motif 4 was unique to the HIR subfamily. Furthermore, there is a high degree of similarity between BnHIR and its cognate AtHIR proteins.

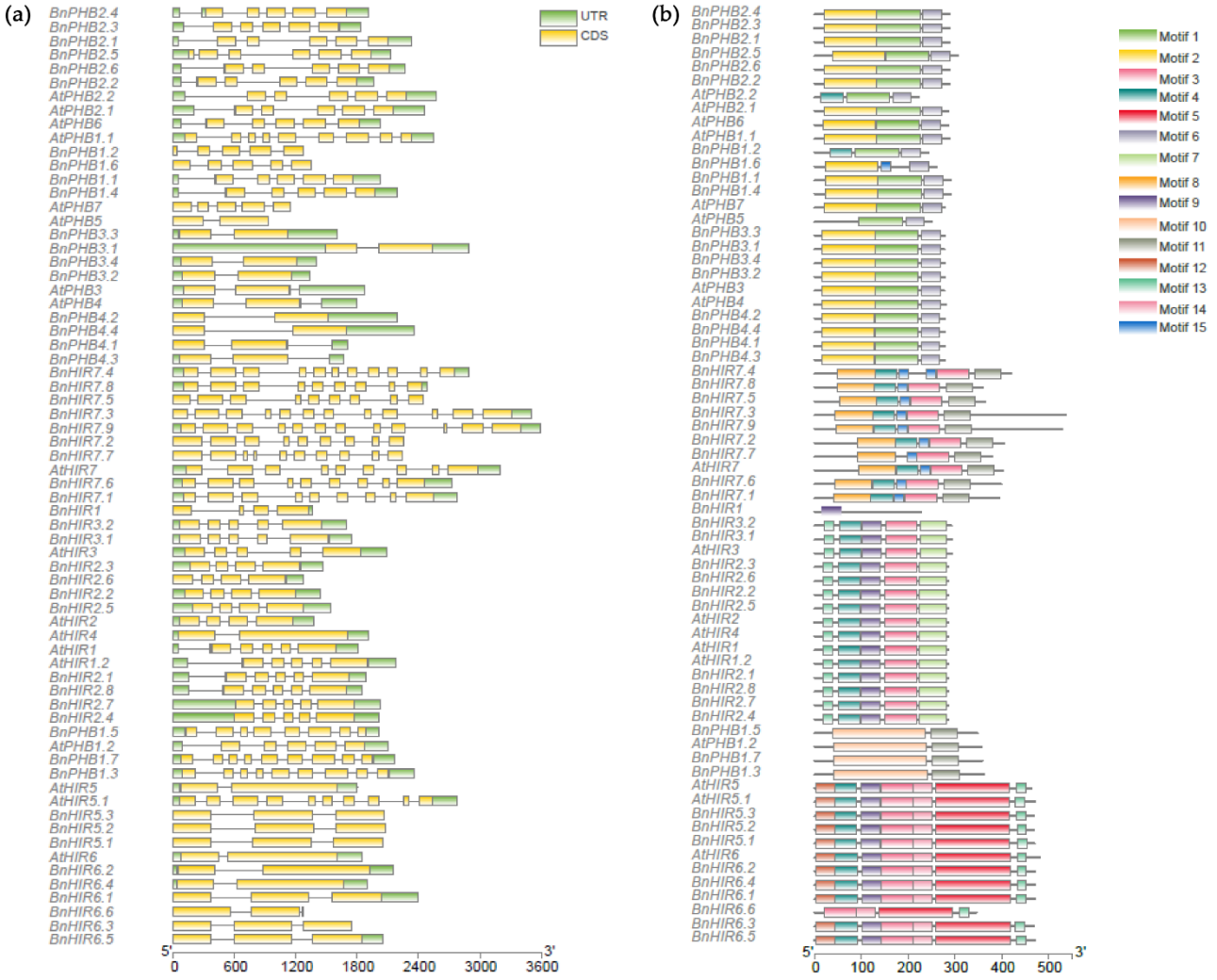

Figure 2. Gene structure and conserved motifs of HIR members in *A. thaliana* and *B. napus*. (**a**) Gene structure is displayed using the Gene Structure Display Server (GSDS 2.0), exons and introns are shown by green boxes and black lines, respectively, and the untranslated regions (UTRs) are indicated by yellow boxes. (**b**) Conserved motifs are identified MEME and represented by differently colored boxes.

3.4. Cis-Acting Elements in the Promoter Regions of BnHIR Genes

To further explore the transcriptional regulation of the *BnHIR* genes, the potential *cis*-acting elements were identified in their upstream 2000 bp genomic DNA sequence. To better understand the potential function of the *BnHIR* genes, *cis*-acting elements involved in light response, defense, and stress response were preserved. All *BnHIR* genes contained light responsiveness, such as GT1-motif and G-box, and at least four *cis*-acting elements were found in the upstream region of each *BnHIR* gene (Figure 3). Elements responsive to phytohormones were also found in most promoter regions of *HIR* genes, including abscisic acid (ABRE) and *cis*-acting regulatory element (CAT-box). Members in Groups 1/2/4 had more abundant *cis*-acting elements, but members in Group 3 had fewer *cis*-acting elements, and *BnPHB1.3* contained only four elements, with no phytohormone and stress *cis*-acting elements. In addition, the promoter regions of *BnHIR* included those *cis*-acting elements, such as the protein binding region (HD-Zip 3), enhancer (CAAT-box), and abiotic stress response (MBS) (Figure S1). Notably, the promoter region of *BnPHB2.4* had the most multitudinous *cis*-acting elements, including 10 phytohormone-responsive elements, 11 light-responsive elements, and six other *cis*-acting elements. In contrast, *BnPHB1.3* had

the fewest *cis*-acting elements in the promoter region, indicating that their functions are conserved or degenerated.

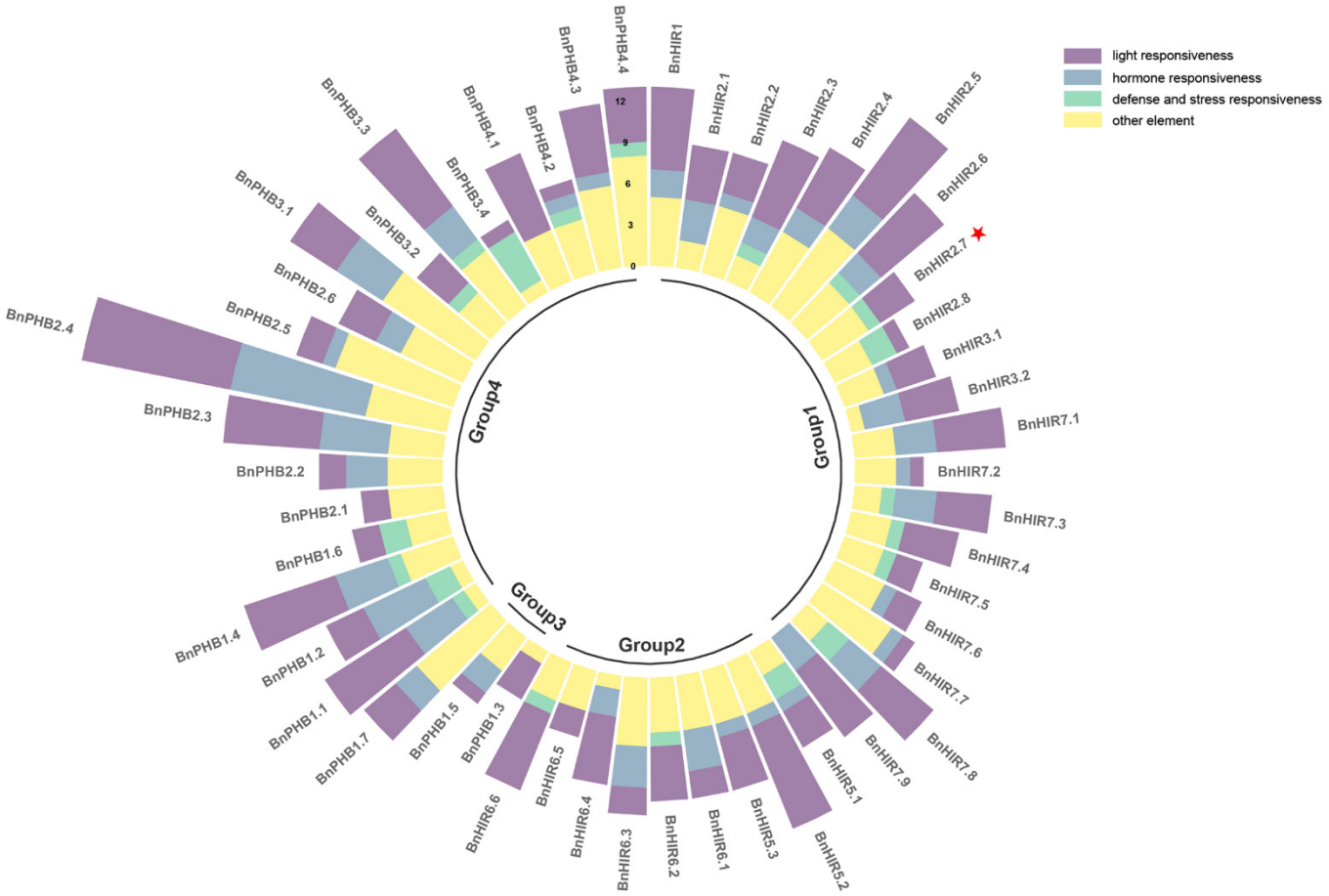

Figure 3. *Cis*-acting elements in the promoter region of *BnHIR* genes. *Cis*-acting elements in promoter regions were predicted using PlantCARE (http://bioinformatics.psb.ugent.be/webtools/plantcare/html/, accessed on 17 March 2022) and plotted using R package tidyverse. All *cis*-acting elements are grouped into four categories and marked with different colored boxes. The red star represents the target gene for subsequent functional verification.

3.5. Expression Patterns of BnHIR Genes at Different Developmental Stages

To better study the biological functions of BnHIRs, we analyzed their expression profiles in numerous tissues during different stages. No expression was detected in *BnHIR2.6*, *BnHIR7.2*, *BnHIR7.7*, *BnPHB1.1*, or *BnPHB1.6* in any examined tissue. In Group 1, *BnHIR2.2* and *BnHIR2.3* were only highly expressed in leaves, and *BnHIR2.7*, *BnHIR3.2*, and *BnHIR3.3* were highly expressed in all detected tissues (Figure 4a). However, *BnHIR7.8*, *BnHIR7.9*, and Group 2 *HIR* genes had little or no expression in various detected tissues. Ten *BnHIR* genes, including *BnHIR2.2*, *BnHIR2.3*, *BnHIR2.5*, *BnHIR2.7*, and *BnHIR2.8*, were highly specifically expressed in leaves, and *BnHIR2.5* and *BnHIR2.7* were also highly specifically and highly expressed in siliques pericarp (Figure 4b). In Group 3, *BnPHB1.7* was expressed in all examined tissues except embryos (Figure 4c). Genes in Group 4 were highly expressed in all tissues, and *BnPHB3.2* and *BnPHB3.3* were higher in seeds and embryos at 43d and 46d (Figure 4d).

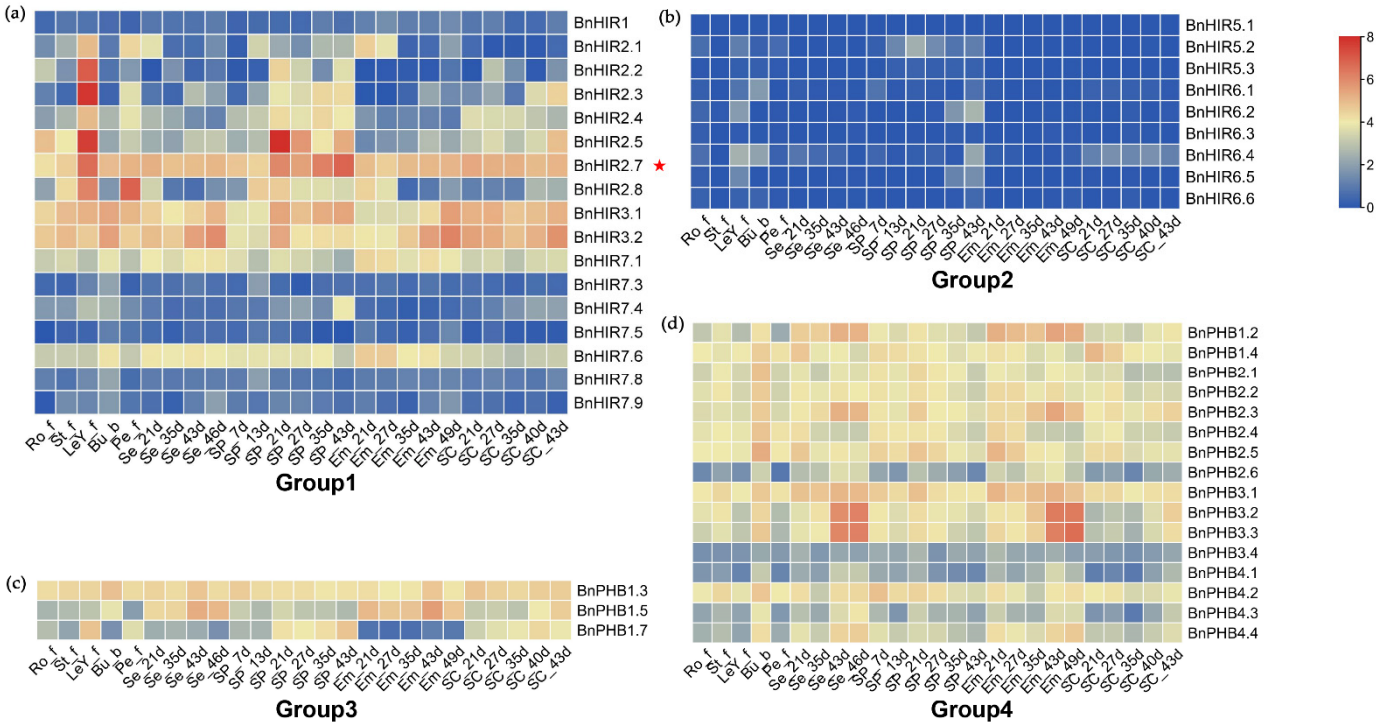

Figure 4. Expression patterns of *BnHIR* genes in different tissues. (**a**) Expression patterns of *HIR* genes in Group 1. (**b**) Expression patterns of *HIR* genes in Group 2. (**c**) Expression patterns of *HIR* genes in Group 3. (**d**) Expression patterns of *HIR* genes in Group 4. The blue-to-red color bar on the right represents $\log_2$-transformed expression values, with blue indicating little or no expression and red indicating high expression. Expression data were obtained from the BrassicaEDB database (https://biodb.swu.edu.cn/brassica/, accessed on 13 February 2022), and expression levels of *BnHIRs* were normalized by $\log_2$(FPKM + 1). Complete tissue names are listed in Materials and Methods. The red star represents the target gene for subsequent functional verification.

3.6. Expression Analysis of BnHIRs under S. sclerotiorum Induction

To further investigate the role of *BnHIRs* under *S. sclerotiorum* induction, we analyzed the expression profiles of *BnHIRs* at different time points in response to *S. sclerotiorum* infection.

HIR genes in Group 1 showed different expression patterns. *BnHIR2.4*, *BnHIR2.5*, *BnHIR3.1*, and *BnHIR3.2* were all highly expressed in the susceptible variety and the resistance variety after *S. sclerotiorum* infection. In particular, *BnHIR2.7* was weakly expressed in the susceptible variety. Still, the expression level in resistant materials was higher and up-regulated rapidly 24 h after infection, reaching a maximum at 48 h and gradually decreasing (Figure 5a). Members in Group 2 had relatively weak responses to *S. sclerotiorum* (Figure 5b). The *PHB* genes in Group 3 were consistently expressed, with no apparent specificity between the two varieties (Figure 5c). As with Group 3, each member of Group 4 had high expression, with no obvious species specificity. However, 48 h after *S. sclerotiorum* infection in the disease-resistant material, all members of Group 4 had a higher response to *S. sclerotiorum* except for *BnPHB2.2*, with the highest expression levels for *BnPHB3* and *BnPHB 4* (Figure 5d).

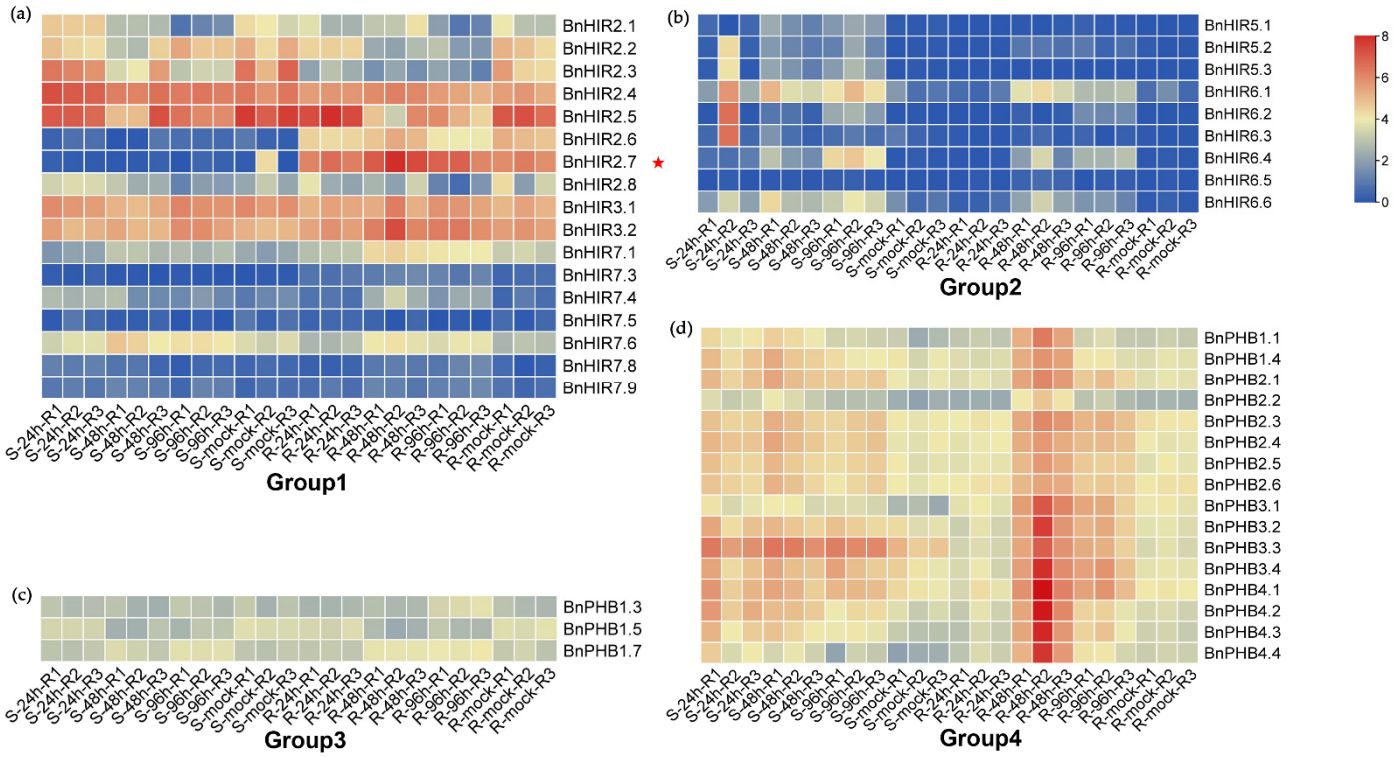

Figure 5. Expression patterns of *BnHIR* genes under *S. sclerotiorum* induction. (**a**) Expression patterns of *HIR* genes in Group 1. (**b**) Expression patterns of *HIR* genes in Group 2. (**c**) Expression patterns of *HIR* genes in Group 3 (**d**) Expression patterns of *HIR* genes in Group 4. The blue-to-red color bar on the right represents the normalized expression value, and expression levels of *BnHIRs* were normalized by $\log_2$(FPKM + 1). Expression data were retrieved from the NCBI SRA database (PRJNA274853). The red star represents the target gene for subsequent functional verification.

3.7. Functional Characterization of BnHIR2.7 in Transgenic Arabidopsis

To further explore the function of *BnHIR2.7*, we detected the phenotype of OV-BnHIR2.7 transgenic *A. thaliana* overexpression lines, Athir2.7-Mu mutants, and wild-type Col-0 plants. The OV-BnHIR2.7-3 line showed the highest BnHIR2.7 expression compared to wild type (Figure S2). Therefore, the OV-BnHIR2.7-3 and Athir2.7-Mu lines were selected for further study.

The expression levels of SA and MeJA pathway marker genes of Col-0, Athir2.7-Mu, and OV-BnHIR2.7 plants were detected at different times after inoculation with *S. sclerotiorum* (Figure S3a). We analyzed the phenotypes of OV-BnHIR2.7 transgenic *A. thaliana* overexpression lines, Athir2.7-Mu mutants, and wild-type Col-0 plants. At the seedling stage, there was no noticeable difference between Col-0 wild-type, OV-*BnHIR2.7*, and Athir2.7-Mu (Figure S3b). At the maturity stage, OV-BnHIR2.7 plants were prominently higher than Athir2.7-Mu plants (Figure S3c). In addition, the siliques of the Col-0 wild-type were prominently smaller than those of the OV-BnHIR2.7 plants but prominently longer than those of the Athir2.7-Mu (Figure S3d). These results suggest that *HIR2.7* is a critical positive regulator of plant growth and development, especially in promoting silique length. Moreover, there was no extreme difference in *BnHIR2.7* expression in the overexpressed lines before and after *S. nucleobium* inoculation (Figure 6a). Notably, trypan blue staining showed that overexpression of *BnHIR2.7* in *A. thaliana* did not induce programmed cell death (Figure 6b). Col-0, Athir2.7-Mu, and OV-BnHIR2.7 *A. thaliana* leaves showed different degrees of lesions at 24 h and 36 h after inoculation with *S. sclerotiorum* (Figure 6c). At 48 h after *S. sclerotiorum* inoculation, the lesions expanded to the entire *A. thaliana* leaf (Figure S3e). Correspondingly, the infected area of strain in overexpressed lines was signifi-

cantly (p = 0.00007) lower than that of Col-0 at 36 h inoculated, and that of Athir2.7-Mu was significantly (p = 0.0036) higher than that of Col-0 at 24 h inoculated (Figure 6d).

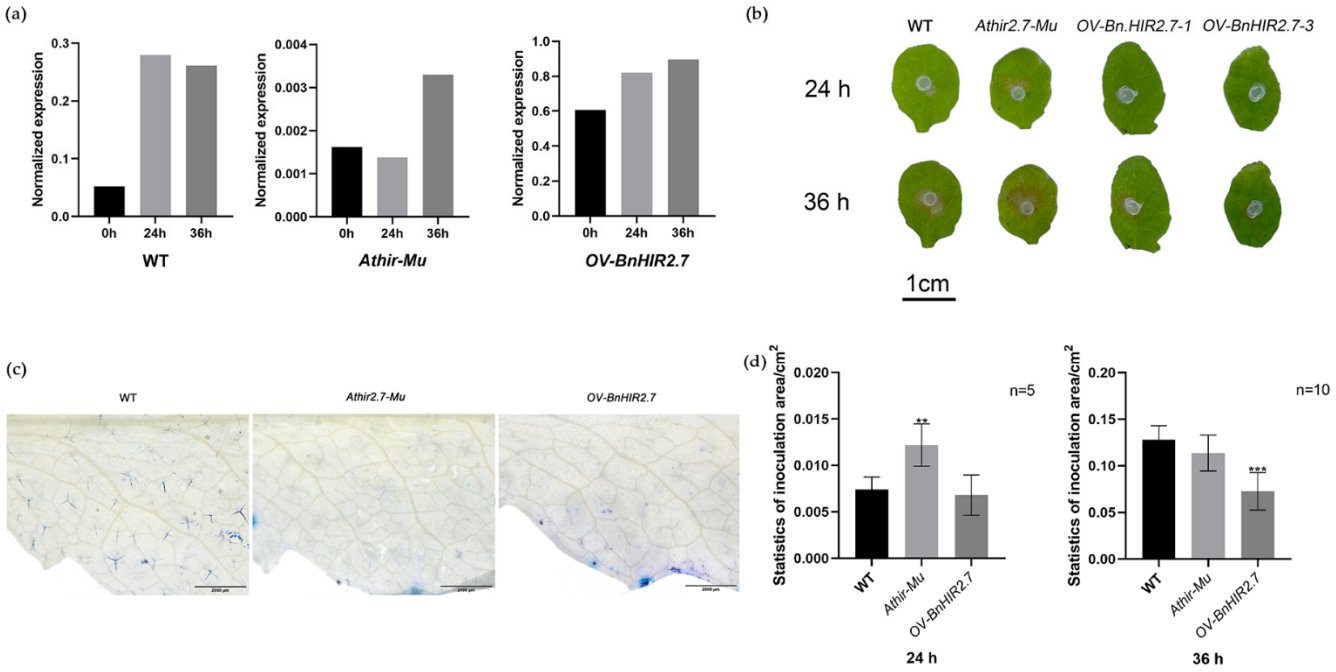

Figure 6. Expression patterns of *BnHIR* subgroup genes induced by *S. sclerotiorum*. (**a**) Expression of Col-0, Athir-Mu, OV-BnHIR2.7 at 24 and 36 h after *S. sclerotiorum* infection. (**b**) Col-0, Athir-Mu, OV-BnHIR2.7 trypan blue staining (image scale 2000 μm). (**c**) Col-0, Athir-Mu, and OV-BnHIR2.7 leaves at 24 and 36 h after inoculation with *S. sclerotiorum*. (**d**) The statistics of the infected area of Col-0, Athir-Mu, OV-BnHIR2.7 at 24 and 36 h after inoculation with *S. sclerotiorum*. Note: ** indicates significant difference at level of $p < 0.01$; *** indicates significant difference at level of $p < 0.001$.

4. Discussion

HIR family genes play key roles in plant development, metabolism, and stress resistance, and they have been identified in many plant species. In wheat, *TaHIR1* and *TaHIR3* expression were reduced in response to environmental stimuli such as low temperature, drought, and high salt stress. *TaHIR1* and *TaHIR3* genes' silencing induced by barley streak mosaic virus reduced the resistance of the wheat variety Suwon11 to the avirulent stripe rust type CYR23 and the necrotic cell region near the infection site and altered the expression levels of defense-related genes [10]. In pepper, overexpression of *CaHIR1* gene resulted in spontaneous cell death, enhanced disease resistance against *P. syringae* [14], and enhanced sensitivity to salinity and drought stress during germination [35]. However, the gene function of *BnHIR* in *B. napus* has not been studied in depth.

Previous studies have shown that *HIR* genes have conserved functions and profound evolutionary origins in each kingdom [7]. It has been reported that 19 and 16 *HIR* genes have been identified in the rice and maize genomes, respectively [7,12]. In this study, we identified 50 *BnHIRs*, and these genes encode HIR proteins with an SPFH or PHB domain, consistent with canonical HIR proteins in other plants [36]. *B. napus* has more *HIR* genes than those plants, probably owing to additional whole-genome triploidy (WGT) during the evolutionary history of *Brassica* crops [15]. In higher plants, *HIR* genes can be divided into four classes, including I (HIR7 clade), II (HIR1/2/3 clade), III (PHB1/2/3/4 clade), and IV (PHB5/6 clade), some of which can be subdivided into smaller subclasses [7,12]. Phylogenetic analysis of the *HIR* genes of *A. thaliana* and *B. napus* was performed. They were divided into four groups according to the bootstrap value, structural and functional characteristics, and named as HIR subfamily (Group 1/2) and PHB (Group 3/4) subfamily, respectively. They were not completely the same as previous studies [11,37]. The *BnHIR*

family genes have relatively diverse gene structure changes (Figure 2a). In addition, the homologous genes in each subfamily have similar characteristics, including gene structure, conserved motifs, and *cis*-acting elements, suggesting their functional conservation (Figure 1). It is predicted that most BnHIR proteins were localized in mitochondria. Furthermore, several *cis*-acting elements have multiple copies in the BnHIR promoter region. This is particularly true for *cis*-acting elements that confer light and hormone responsiveness, which would enhance the response of the *BnHIR* gene to stress and developmental signals, and suggests that the *BnHIR* gene plays an important role in these processes. Furthermore, in *B. napus*, there are more members in Groups 1 and 4 than in Groups 2 and 3, suggesting that the ancestral evolutionary branch of Group 1/4 has undergone more expansion than the other two evolutionary branches. *BnPHB1.3*, *BnPHB1.5*, and *BnPHB1.7* corresponded to *AtPHB1.2* and independently became Group 3 in the phylogenetic tree, and they were not divided into the same group with other *BnPHBs* (Figure 1). This may indicate that the *HIR* genes in *B. napus* have differentiated and performed different functions.

The expression pattern of *HIR* genes has been studied in several species. In maize, the expression pattern was classified into three groups, A, B, and C, based on the results of cluster analysis. The expression of *HIR* genes in Group A was higher in the embryo and stem. *HIR* genes in Group B may play an important role in seed development, while *HIR* genes in Group C may alter the development and senescence of maize [12]. In *B. napus*, *BnPHB3.2* and *BnPHB3.3* in Group 4 were also highly expressed in seeds and embryos, suggesting that *HIR* genes play a considerable role in embryo and seed development. In soybean, *GmHIR1* is highly expressed in flower buds, while *GmHIR2* is mainly expressed in globular embryos. The majority of the *BnHIR* genes are not active in buds, which may be due to the function degradation in *B. napus*. In the *GmHIR15* and *GmHIR16* gene pair, the expression of *GmHIR15* in leaves increased to a higher level than that of GmHIR16. In the *GmHIR14* and *GmHIR17* gene pair, *GmHIR14* was expressed in seeds, but *GmHIR17* was not [38]. This is basically consistent with the function of the *BnHIR* genes. Furthermore, in tomato (*Solanum lycopersicum* L.), the expression pattern of tomato *SlHIR* genes is spatially specific; for example, *SlPHB4* and *SlPHB10* were expressed in root and flower tissues, respectively. *SlPHB8* and *SlPHB9* were highly expressed in 2 cm fruit, while the expression patterns of *SlPHB5*, *SlPHB14*, and *SlPHB15* increased with the fruit development stages [35]. In our study, most members of the *BnHIR2/3* and *BnPHB2/3* subfamilies were highly expressed in seeds, seed coats, and embryos during seed development and siliques during maturation. *HIR* genes were highly expressed in seeds and siliques in several species, suggesting that these genes have important roles in seed development and maturation. Compared with other species, however, the *HIR* gene in *B. napus* appears to have lost its function in promoting root development and promoting flowering. After inoculation with *S. sclerotiorum*, the comparison of gene expression between the two materials found that the expression levels of 31 *HIR* genes were up-regulated at 48 h and 96 h (Figure S4c), while that of nine *HIR* genes were down-regulated (Figure S4d), suggesting that most of the *HIR* genes had a positive response to the induction of *S. sclerotiorum*.

Some studies have been conducted on the function and mechanism of the *HIR* gene. *AtPHB3* and *AtPHB4* are mainly expressed in shoot and proliferative root tissues, and overexpressed *AtPHB3* and *AtPHB4* exhibit an irregular leaf shape and extensive branching phenotype [39,40]. It has been reported that *NbPHB1* and *NbPHB2* are prominently reduced during plant senescence. This may be because HIR proteins interact directly or indirectly with mitochondrial DNA (mtDNA) at the molecular level to regulate reactive oxygen species' (ROS) formation and oxidative phosphorylation (OXPHOS) [41–44]. HIR proteins may also be involved in the mitochondrial organization [45,46]. *Athir2-1* and *Athir3-1* mutants allow normal growth of *Pto* DC3000 AvrRpt2 but not *Pto* DC3000, and overexpression of *AtHIR1* and *AtHIR2* reduces *Pto* DC3000 growth [8]. In rice, overexpression of *OsHIR1* could make plants more susceptible to hypersensitivity, resulting in a faster response to restrict the development of invading pathogens from the site of infection to otherwise healthy tissue [9]. Overexpression of *CaHIR1* in pepper enhances basal resistance to infection by

hemi-biotrophic bacteria or biotrophic oomycete pathogens [33]. Compared with Col-0, the lesion area of *OV-BnHIR2.7 A. thaliana* leaves was smaller, while *Athir2.7-Mu A. thaliana* leaves lesions expanded. These results indicate that when the expression level of *BnHIR2.7* was low or silenced, plants could not effectively defend against *S. sclerotiorum* infection (Figure 6c). In addition, qRT-PCR results show that Col-0, *OV-BnHIR2.7*, and *Athir2.7-Mu A. thaliana* were prominently up-regulated after inoculation with *S. sclerotiorum*, suggesting that *BnHIR2.7* responds to *S. sclerotiorum*. In addition to resistance to *S. sclerotiorum*, the *A. thaliana Athir2.7-Mu* and *OV-BnHIR2.7* lines showed differences in biomass (Figure S3c) and silique size (Figure S3d) compared with Col-0. This may imply that *BnHIR2.7* may be a potential gene with disease resistance and improved crop yield. In recent years, a series of investigations have been performed to study SD resistance in *B. napus*. Several transcription factors and kinases have been revealed to be associated with SD resistance signaling pathways, such as *BnWRKY33* [47,48], *BNWRKY 70* [49], and *BnMPK3* [50]. In addition, rapid alkalinization factors (RALF), such as *BnRALF10*, induce multiple immune responses to exhibit resistance to *S. sclerotiorum*, including ROS accumulation, cytoplasmic Ca^{2+} promotion, and defense-related gene expression induction [51]. It has also been speculated that Phloem proteins (PP2s) can cross-link together through disulfide bonds to form high molecular weight polymers, which block the sieve to form a physical barrier to slow mycelial colonization [1]. As a potential gene family for disease resistance, *HIR* may be located upstream of SA- and MeJA-related pathways and inhibit the spread of *S. sclerotiorum* by promoting the accumulation of SA and H_2O_2 in the plant [14]. To clarify the possible mechanism of *BnHIR2.7* disease resistance, we quantitatively analyzed the key genes of SA and MeJA pathways before and after *S. sclerotiorum* inoculation. qRT-PCR results showed that marker gene expressions in the SA and MeJA pathways were up-regulated, respectively, after heterologous overexpression of *BnHIR2.7 Arabidopsis* was inoculated with *S. sclerotiorum* (Figure S3a), suggesting that *HIR* responds to biotic stress through, but not dependent on, SA or JA pathways. Next, further experiments will reveal the mechanisms of *BnHIR2.7* to *S. sclerotiorum* resistance.

5. Conclusions

In this study, 50 *BnHIR* genes were identified in the *B. napus* genome based on publicly available genomic data. The identified *BnHIR* genes were phylogenetically divided into four groups, and their evolutionary relationships were analyzed. Under normal growth conditions, the majority of the *BnHIR* genes in Group 1 and Group 4 were highly expressed in leaves, siliques, embryos, and seeds. The *HIR* gene in Group 2 was low or not expressed in the detected tissues. Except for *BnPHB1.7*, other genes of Group 3 had high expression levels in the detected tissues. Following inoculation with *S. sclerotiorum*, the majority of the *HIR* genes in Group 1 and Group 4 were up-regulated. *BnHIR2.7* was barely expressed in the susceptible cultivars but highly expressed in resistant materials. We experimentally verified that overexpression of *BnHIR2.7* could inhibit the growth of *S. sclerotiorum*. In addition, our study found the role of *BnHIR2.7* in promoting silique, which also provides clues for further research. These results may suggest further functional characterization of the *BnHIR* gene family of great value, especially when considering genetic improvements for agronomic traits and *S. sclerotiorum* resistance in *B. napus*.

Supplementary Materials: The following supporting information can be downloaded at: https://www.mdpi.com/article/10.3390/horticulturae8100874/s1, Figure S1: Statistics of *cis*-acting elements in the *BnHIR* promoter region. Figure S2: Relative expression level of *Arabidopsis* transgenic lines. Figure S3: Phenotype comparison of wild type, *Athir2.7-Mu*, and *OV-BnHIR2.7* lines. Figure S4: Venn diagram of changes in *HIR* gene expression under *Sclerotinia sclerotiorum* infection; Table S1: Primers used in this study.

Author Contributions: J.L. and K.L.: conceptualization, methodology, and funding acquisition; M.L. and Y.T.: performed the sampling and experiments, writing—original draft preparation; M.Y. and Y.F.: contributed to data analysis and interpretation; S.U.K., W.C. and S.W.: validation; X.L., L.W. and

W.C.: software; C.Q.: supervision. K.L.: writing—reviewing and editing. All authors have read and agreed to the published version of the manuscript.

Funding: This work was supported by the National Natural Science Foundation of China [31871653 and 32272111 to K.L.], the Talent Project of Chongqing Natural Science Foundation [cstc2021ycjh-bgzxm0033 to K.L.], and Germplasm Creation Special Program of Southwest University.

Data Availability Statement: Not applicable.

Conflicts of Interest: The authors declare that the research was conducted in the absence of any commercial or financial relationships that could be construed as a potential conflict of interest.

Abbreviations

HIR: hypersensitive-induced response protein; SD, Sclerotinia disease; *B. napus*, *Brassica napus*; *S. sclerotiorum*, *Sclerotinia sclerotiorum*; *A. thaliana*: *Arabidopsis thaliana*; MS: Murashige and Skoog medium; PDA: Potato Dextrose Agar; qRT-PCR: quantitative real-time PCR; SPFH, stomatin/prohibitin/flotillin/HflK domain; JA, jasmonic acid; MeJA, methyl jasmonate; WGT, whole-genome triploidy; ROS, reactive oxygen species; SA, salicylic acid; RPS2, resistant to *P. syringae* 2; ABA, abscisic acid; GA, gibberellin; CDS, the coding sequence; BLASTP, basic local alignment search tool protein; pI, theoretical isoelectric point; MW, molecular weight; kDa, kilodalton; MUSCLE, multiple sequence comparison by log-expectation; MEME, Multiple EM for Motif Elicitation; ML, maximum likelihood; CTAB, cetyl trimethyl ammonium bromide; MIQE, Minimum Information for Publication of Quantitative Real-Time PCR experiments; ABRE, abscisic acid responsiveness; GARE, gibberellin responsiveness; Col-0, Columbia; WGT, whole-genome triploidization; *B. rapa*, *Brassica rapa*; *B. oleracea*, *Brassica oleracea*.

References

1. Zuo, R.; Xie, M.; Gao, F.; Sumbal, W.; Cheng, X.; Liu, Y.; Bai, Z.; Liu, S. The Characterization of the *Phloem Protein 2* Gene Family Associated with Resistance to *Sclerotinia sclerotiorum* in *Brassica napus*. *Int. J. Mol. Sci.* **2022**, *23*, 3934. [CrossRef]
2. Ding, L.; Li, T.; Guo, X.; Li, M.; Liu, X.; Cao, J.; Tan, X. Sclerotinia Stem Rot Resistance in Rapeseed: Recent Progress and Future Prospects. *J. Agric. Food Chem.* **2021**, *69*, 2965–2978. [CrossRef]
3. Nadimpalli, R.; Yalpani, N.; Johal, G.S.; Simmons, C.R. Prohibitins, Stomatins, and Plant Disease Response Genes Compose a Protein Superfamily That Controls Cell Proliferation, Ion Channel Regulation, and Death. *J. Biol. Chem.* **2000**, *275*, 29579–29586. [CrossRef] [PubMed]
4. Atkinson, M.M.; Keppler, L.D.; Orlandi, E.W.; Baker, C.J.; Mischke, C.F. Involvement of Plasma-Membrane Calcium Influx in Bacterial Induction of the K^+/H^+ And Hypersensitive Responses in Tobacco. *Plant Physiol.* **1990**, *92*, 215–221. [CrossRef]
5. Beers, E.P.; McDowell, J.M. Regulation and Execution of Programmed Cell Death in Response to Pathogens, Stress and Developmental Cues. *Curr. Opin. Plant Biol.* **2001**, *4*, 561–567. [CrossRef]
6. Lam, E.; Kato, N.; Lawton, M. Programmed cell death, mitochondria and the plant hypersensitive response. *Nature* **2001**, *411*, 848–853. [CrossRef]
7. Di, C.; Xu, W.; Su, Z.; Yuan, J.S. Comparative Genome Analysis of *PHB* Gene Family Reveals Deep Evolutionary Origins and Diverse Gene Function. *BMC Bioinform.* **2010**, *11*, S22. [CrossRef]
8. Qi, Y.; Tsuda, K.; Nguyen, L.V.; Wang, X.; Lin, J.; Murphy, A.S.; Glazebrook, J.; Thordal-Christensen, H.; Katagiri, F. Physical Association of *Arabidopsis* Hypersensitive Induced Reaction Proteins (Hirs) with the Immune Receptor RPS2. *J. Biol. Chem.* **2011**, *286*, 31297–31307. [CrossRef]
9. Zhou, L.; Cheung, M.Y.; Li, M.W.; Fu, Y.; Sun, Z.; Sun, S.M.; Lam, H.M. Rice Hypersensitive Induced Reaction Protein 1 (OsHIR1) Associates with Plasma Membrane and Triggers Hypersensitive Cell Death. *BMC Plant Biol.* **2010**, *10*, 290. [CrossRef]
10. Duan, Y.; Guo, J.; Shi, X.; Guan, X.; Liu, F.; Bai, P.; Huang, L.; Kang, Z. Wheat Hypersensitive-Induced Reaction Genes *Tahir1* and *Tahir3* Are Involved in Response to Stripe Rust Fungus Infection and Abiotic Stresses. *Plant Cell Rep.* **2012**, *32*, 273–283. [CrossRef]
11. Karrer, E.E.; Beachy, R.N.; Holt, C.A. Cloning of Tobacco Genes That Elicit the Hypersensitive Response. *Plant Mol. Biol.* **1998**, *36*, 681–690. [CrossRef] [PubMed]
12. Wen, X.; Niu, T.; Kong, X. In Silico Analysis of *PHB* Gene Family in Maize. *Plant Growth Regul.* **2013**, *73*, 181–191. [CrossRef]
13. Rostoks, N.; Schmierer, D.; Kudrna, D.; Kleinhofs, A. Barley Putative Hypersensitive Induced Reaction Genes: Genetic Mapping, Sequence Analyses and Differential Expression in Disease Lesion Mimic Mutants. *Theor. Appl. Genet.* **2003**, *107*, 1094–1101. [CrossRef]
14. Jung, H.W.; Hwang, B.K. The Leucine-Rich Repeat (LRR) Protein, Calrr1, Interacts with the Hypersensitive Induced Reaction (HIR) Protein, Cahir1, and Suppresses Cell Death Induced by the Cahir1 Protein. *Mol. Plant Pathol.* **2007**, *8*, 503–514. [CrossRef]

15. Chalhoub, B.; Denoeud, F.; Liu, S.; Parkin, I.A.P.; Tang, H.; Wang, X.; Chiquet, J.; Belcram, H.; Tong, C.; Samans, B.; et al. Early Allopolyploid Evolution in the Post-Neolithic *Brassica napus* Oilseed Genome. *Science* **2014**, *345*, 950–953. [CrossRef]
16. Altschul, S.F.; Gish, W.; Miller, W.; Myers, E.W.; Lipman, D.J. Basic Local Alignment Search Tool. *J. Mol. Biol.* **1990**, *215*, 403–410. [CrossRef]
17. Altschul, S.F.; Madden, T.L.; Schaffer, A.A.; Zhang, J.H.; Zhang, Z.; Miller, W.; Lipman, D.J. Gapped BLAST and PSI-BLAST: A New Generation of Protein Database Search Programs. *Nucleic Acids Res.* **1997**, *25*, 3389–3402. [CrossRef]
18. Fan, Y.; Yu, M.; Liu, M.; Zhang, R.; Sun, W.; Qian, M.; Duan, H.; Chang, W.; Ma, J.; Qu, C.; et al. Genome-Wide Identification, Evolutionary and Expression Analyses of the *GALACTINOL SYNTHASE* Gene Family in Rapeseed and Tobacco. *Int. J. Mol. Sci.* **2017**, *18*, 2768. [CrossRef]
19. Chou, K.C.; Shen, H.B. Plant-mPLoc: A Top-Down Strategy to Augment the Power for Predicting Plant Protein Subcellular Localization. *PLoS ONE* **2010**, *5*, e11335. [CrossRef]
20. Edgar, R.C. MUSCLE: Multiple Sequence Alignment with High Accuracy and High Throughput. *Nucleic Acids Res.* **2004**, *32*, 1792–1797. [CrossRef]
21. Guindon, S.; Dufayard, J.F.; Lefort, V.; Anisimova, M.; Hordijk, W.; Gascuel, O. New Algorithms and Methods to Estimate Maximum-Likelihood Phylogenies: Assessing the Performance of PhyML 3.0. *Syst. Biol.* **2010**, *59*, 307–321. [CrossRef] [PubMed]
22. Lefort, V.; Longueville, J.E.; Gascuel, O. SMS: Smart Model Selection in PhyML. *Mol. Biol. Evol.* **2017**, *34*, 2422–2424. [CrossRef] [PubMed]
23. Subramanian, B.; Gao, S.; Lercher, M.J.; Hu, S.; Chen, W.H. Evolview v3: A Webserver for Visualization, Annotation, and Management of Phylogenetic Trees. *Nucleic Acids Res.* **2019**, *47*, W270–W275. [CrossRef] [PubMed]
24. Bailey, T.L.; Williams, N.; Misleh, C.; Li, W.W. MEME: Discovering and Analyzing DNA and Protein Sequence Motifs. *Nucleic Acids Res.* **2006**, *34*, W369–W373. [CrossRef] [PubMed]
25. Chen, C.; Chen, H.; Zhang, Y.; Thomas, H.R.; Frank, M.H.; He, Y.; Xia, R. TBtools: An Integrative Toolkit Developed for Interactive Analyses of Big Biological Data. *Mol. Plant.* **2020**, *13*, 1194–1202. [CrossRef] [PubMed]
26. Lescot, M.; Dehais, P.; Thijs, G.; Marchal, K.; Moreau, Y.; Van de Peer, Y.; Rouze, P.; Rombauts, S. PlantCARE, a Database of Plant *Cis*-Acting Regulatory Elements and a Portal to Tools for In Silico Analysis of Promoter Sequences. *Nucleic Acids Res.* **2002**, *30*, 325–327. [CrossRef]
27. Chao, H.; Li, T.; Luo, C.; Huang, H.; Ruan, Y.; Li, X.; Niu, Y.; Fan, Y.; Sun, W.; Zhang, K.; et al. BrassicaEDB: A Gene Expression Database for *Brassica* Crops. *Int. J. Mol. Sci.* **2020**, *21*, 5831. [CrossRef]
28. Abedi, A.; Hajiahmadi, Z.; Kordrostami, M.; Esmaeel, Q.; Jacquard, C. Analyses of *Lysin-motif Receptor-like Kinase* (*LysM*-RLK) Gene Family in Allotetraploid *Brassica napus* L. and Its Progenitor Species: An In Silico Study. *Cells* **2021**, *11*, 37. [CrossRef]
29. Porebski, S.; Bailey, L.G.; Baum, B.R. Modification of a CTAB DNA Extraction Protocol for Plants Containing High Polysaccharide and Polyphenol Components. *Plant Mol. Biol. Rep.* **1997**, *15*, 8–15. [CrossRef]
30. Schmidt, R.; Willmitzer, L. High Efficiency *Agrobacterium tumefaciens*-Mediated-Transformation of *Arabidopsis thaliana* Leaf and Cotyledon Explants. *Plant Cell Rep.* **1988**, *7*, 583–586. [CrossRef]
31. Lu, K.; Li, T.; He, J.; Chang, W.; Zhang, R.; Liu, M.; Yu, M.; Fan, Y.; Ma, J.; Sun, W.; et al. qPrimerDB: A Thermodynamics-Based Gene-Specific Qrt-PCR Primer Database for 147 Organisms. *Nucleic Acids Res.* **2018**, *46*, D1229–D1236. [CrossRef] [PubMed]
32. Bustin, S.A.; Benes, V.; Garson, J.A.; Hellemans, J.; Huggett, J.; Kubista, M.; Mueller, R.; Nolan, T.; Pfaffl, M.W.; Shipley, G.L.; et al. The MIQE Guidelines: Minimum Information for Publication of Quantitative Real-Time PCR Experiments. *Clin. Chem.* **2009**, *55*, 611–622. [CrossRef] [PubMed]
33. Wu, G.; Zhang, L.; Wu, Y.; Cao, Y.; Lu, C. Comparison of Five Endogenous Reference Genes for Specific PCR Detection and Quantification of *Brassica napus*. *J. Agric. Food Chem.* **2010**, *58*, 2812–2817. [CrossRef] [PubMed]
34. Swift, M.L. GraphPad Prism, Data Analysis, and Scientific Graphing. *J. Chem. Inf. Comput. Sci.* **1997**, *37*, 411–412. [CrossRef]
35. Jung, H.W.; Lim, C.W.; Lee, S.C.; Choi, H.W.; Hwang, C.H.; Hwang, B.K. Distinct Roles of the Pepper Hypersensitive Induced Reaction Protein Gene *Cahir1* in Disease and Osmotic Stress, as Determined by Comparative Transcriptome and Proteome Analyses. *Planta* **2008**, *227*, 409–425. [CrossRef]
36. Morrow, I.C.; Parton, R.G. Flotillins and the PHB Domain Protein Family: Rafts, Worms and Anaesthetics. *Traffic* **2005**, *6*, 725–740. [CrossRef]
37. Huang, F.; Ye, X.; Wang, Z.; Ding, Y.; Cai, X.; Yu, L.; Waseem, M.; Abbas, F.; Ashraf, U.; Chen, X.; et al. The *prohibitins* (*PHB*) Gene Family in Tomato: Bioinformatic Identification and Expression Analysis Under Abiotic and Phytohormone Stresses. *GM Crop. Food* **2021**, *12*, 535–550. [CrossRef]
38. Song, M.; Peng, X.; Du, C.; Lei, L.; Zhang, T.; Xiang, Y. Genome-Wide Analysis of the *PHB* Gene Family in *Glycine max* (L.). *Merr. Genes Genom.* **2017**, *39*, 1095–1106. [CrossRef]
39. Van Aken, O.; Pečenková, T.; van de Cotte, B.; De Rycke, R.; Eeckhout, D.; Fromm, H.; De Jaeger, G.; Witters, E.; Beemster, G.T.; Inzé, D.; et al. Mitochondrial Type-I Prohibitins of *Arabidopsis thaliana* are required for Supporting Proficient Meristem Development. *Plant J.* **2007**, *52*, 850–864. [CrossRef]
40. Wang, Y.; Ries, A.; Wu, K.; Yang, A.; Crawford, N.M. The *Arabidopsis* prohibitin Gene *PHB3* Functions in Nitric Oxide-Mediated Responses and in Hydrogen Peroxide-Induced Nitric Oxide Accumulation. *Plant Cell* **2010**, *22*, 249–259. [CrossRef]

41. Artal-Sanz, M.; Tsang, W.Y.; Willems, E.M.; Grivell, L.A.; Lemire, B.D.; van der Spek, H.; Nijtmans, L.G. The Mitochondrial Prohibitin Complex Is Essential for Embryonic Viability and Germline Function in *Caenorhabditis elegans*. *J. Biol. Chem.* **2003**, *278*, 32091–32099. [CrossRef]
42. Chen, J.C.; Jiang, C.Z.; Reid, M.S. Silencing a Prohibitin Alters Plant Development and Senescence. *Plant J.* **2005**, *44*, 16–24. [CrossRef]
43. Ahn, C.S.; Lee, J.H.; Reum Hwang, A.; Kim, W.T.; Pai, H.S. Prohibitin is Involved in Mitochondrial Biogenesis in Plants. *Plant J.* **2006**, *46*, 658–667. [CrossRef]
44. Artal-Sanz, M.; Tavernarakis, N. Prohibitin Couples Diapause Signalling to Mitochondrial Metabolism During Ageing in *C. elegans*. *Nature* **2009**, *461*, 793–797. [CrossRef]
45. Merkwirth, C.; Langer, T. Prohibitin Function Within Mitochondria: Essential Roles for Cell Proliferation and Cristae Morphogenesis. *Biochim. Biophys. Acta* **2009**, *1793*, 27–32. [CrossRef]
46. Merkwirth, C.; Dargazanli, S.; Tatsuta, T.; Geimer, S.; Löwer, B.; Wunderlich, F.T.; von Kleist-Retzow, J.C.; Waisman, A.; Westermann, B.; Langer, T. Prohibitins Control Cell Proliferation and Apoptosis by Regulating OPA1-Dependent Cristae Morphogenesis in Mitochondria. *Genes* **2008**, *22*, 476–488. [CrossRef]
47. Wang, Z.; Fang, H.; Chen, Y.; Chen, K.; Li, G.; Gu, S.; Tan, X. Overexpression of *BnWRKY33* in Oilseed Rape Enhances Resistance to *Sclerotinia sclerotiorum*. *Mol. Plant Pathol.* **2015**, *15*, 677–689. [CrossRef]
48. Hu, H.; Tang, Y.; Wu, J.; Chen, F.; Yang, Y.; Pan, X.; Dong, X.; Jin, X.; Liu, S.; Du, X. *Brassica napus* Mediator Subunit16 Induces *BnMED25*- and *BnWRKY33*-Activated Defense Signaling to Confer *Sclerotinia sclerotiorum* Resistance. *Front. Plant Sci.* **2021**, *12*, 663536. [CrossRef]
49. Sun, Q.; Lin, L.; Liu, D.; Wu, D.; Fang, Y.; Wu, J.; Wang, Y. CRISPR/Cas9-Mediated Multiplex Genome Editing of the *BnWRKY11* and *BnWRKY70* Genes in *Brassica napus* L. *Int. J. Mol. Sci.* **2018**, *19*, 2716. [CrossRef]
50. Wang, Z.; Bao, L.; Zhao, F.; Tang, M.; Chen, T.; Li, Y.; Wang, B.; Fu, B.; Fang, H.; Li, G.; et al. *BnaMPK3* Is a Key Regulator of Defense Responses to the Devastating Plant Pathogen *Sclerotinia sclerotiorum* in Oilseed Rape. *Front. Plant Sci.* **2019**, *10*, 91. [CrossRef]
51. He, Y.; Zhang, Z.; Xu, Y.; Chen, S.; Cai, X. Genome-Wide Identification of Rapid Alkalinization Factor Family in *Brassica napus* and Functional Analysis of *BnRALF10* in Immunity to *Sclerotinia sclerotiorum*. *Front. Plant Sci.* **2022**, *3*, 877404. [CrossRef]